

QUANTITATIVE ANALYSIS OF SAUSAGING IN NB BARRIER CLAD FILAMENTS OF NB-46.5WT% TIAS A FUNCTION OF FILAMENT DIAMETER AND HEAT TREATMENT

Y. E. High[†], P. J. Lee[†], J. C. McKinnell*, D. C. Larbalestier[†]

[†]University of Wisconsin-Madison, Applied Superconductivity Center, Madison, WI

*Superconductor Development Division, TWCA, Albany, OR

ABSTRACT

Image processing techniques were used to determine the amount of sausaging occurring in advanced barrier-clad Nb-46.5 wt. %Ti multifilament superconducting wires. The standard deviation of the filament cross sectional area divided by the mean cross-sectional area (σ_{n-1}/\bar{A}) increased with decreasing final filament diameter and increasing heat treatment temperature and duration. The underlying control factor was the breakdown of the Nb diffusion barrier during heat treatment. A 2 % barrier was found inadequate to protect filaments of 6 μm diameter under aggressive heat treatment conditions. When the barrier was significantly breached, hard intermetallics grew in the filament-matrix interface region. The filament cross-sectional uniformity, the transport critical current density and the resistive transition index (n) all declined when the barrier was breached. More extended heat treatments produced higher intrinsic critical current densities, but their benefit was negated when the barrier was too thin.

INTRODUCTION

The specifications for the Superconducting Super Collider (SSC) conductor are very demanding. During the R&D phase there has been a continual push to develop higher critical current density (J_c), finer filaments, longer piece lengths greater yields and higher end-to-end wire uniformity¹⁻³. One of the crucial practical concerns is to avoid significant filament sausaging. Sausaging is the term used to describe the variation in filament diameter along the length of the wire. The extrinsic factor that is most responsible for sausaging has been the formation of Cu-Nb-Ti intermetallics at the superconductor-Cu interface.⁴⁻⁷ These intermetallics are hard and brittle and do not deform uniformly with the filament during wire drawing, thus producing local filament necking. In recognition of this problem, a Nb diffusion barrier is now widely used to deter intermetallic formation⁸. Although filament sausaging has been greatly reduced by the addition of a Nb barrier, it has not yet been avoided completely. Its dependence on additional variables, such as the length, number, time of heat treatment and final filament diameter has not yet been clarified. In practice the transport critical current density, J_{ct} , is always maximized when there is some sausaging⁹. However a reliable production process must bring this under control and make the filament sausaging process predictable.

Prior experiments conducted in this group^{10,11} have shown that there is an increase in filament sausaging as the wire diameter decreases and the final drawing strain is increased. This effect can also be followed by measuring the resistive transition index n . Wames and Larbalestier^{10,11} and Ekin¹² tried to connect the area non-uniformity of the filaments to the critical current distribution in the wire. What is clearly evident from all of these studies is that a high quality composite is one in which the intrinsic critical current density (i.e. the flux pinning J_c) is maximized by heat treatments which produce a large density of α -Ti precipitates⁹, without the process initiating significant filament sausaging. The history of the SSC conductor development is one in which success in improving any one property (e.g. the J_c at 9 μm filament diameter) immediately led to the push to improve J_{ct} at even finer filament sizes.

In this study we set out to quantify these effects. We compared the behavior of both 9 μm and 6 μm diameter SSC R&D conductors to a significantly larger (20 μm diameter) Fermilab Quadrupole conductor. The processing of the composites was varied from the very gentle to the very aggressive and the resulting impact on the degree of filament sausing, the breadth of the resistive transition and the J_{ct} was measured. The results show that there is a very direct coupling between these parameters. A companion paper by Faase et al. explicitly studies the diffusional breakdown of the Nb barrier¹³.

EXPERIMENTAL APPROACH

Multifilament rods were received from three different companies, IGC, OST and Supercon. The rods were industrially processed to a diameter of approximately 1 inch. From the total of 14 wires received, 6 were chosen for this experiment. (Table 1).

The wire heat treatments and processing from the nominal 1 inch dia. down were conducted in our laboratory. Three different heat treatments were selected. The A heat treatment was very gentle. It was designed to give an anneal to the copper, while inducing minimum precipitation in the Nb-Ti. It consisted of 3 heat treatments of 3 hours at 300 °C. It was previously determined that only 3% α -Ti forms during this heat treatment¹⁴. The B heat treatment approximates a standard industrially used schedule and consists of 3 heat treatments of 40 hours at 375 °C, which produce about 15% of α -Ti. The C heat treatment was an aggressive one. It utilized 3 heat treatments of 80 hours at 420 °C and would be expected to produce about 20 % of α -Ti. This heat treatment has previously been shown to give optimum intrinsic J_c ¹⁵. Each of these heat treatments was given at the nominal 1 inch size, at 0.6 inch and at 0.325 inch diameter. The wire deformation is reported in terms of true strain ϵ , where $\epsilon = 2 \ln [D_0/D]$, where D_0 is the extrusion diameter and D is the wire size.

Samples for image analysis were taken after each heat treatment and at various steps in the final drawing process. The samples were mounted, ground and polished with special care so as to minimize scratches and surface irregularity, which complicate the image processing. We found that enchants could not be employed, since they produced grain contrast in the Cu, thus degrading the contrast between the matrix and Nb-Ti filaments. The video image from the microscope was fed directly into the image analyzer. The system used has 1024 \times 1024 resolution and a variety of standard contrast level and edge enhancement capabilities. Typically about 80-100 filaments were examined at a time. The specific variables of interest were the mean filament cross sectional area (\bar{A}) and the standard deviation about the mean (σ_{n-1}). The image analyzer was also used to count the number of filaments present and to determine the maximum and minimum filament area for each analyzed region.

Transport critical current densities were measured in standard fashion¹⁰. J_{ct} was determined at a resistivity of $10^{-14} \Omega\cdot\text{m}$. The resistive transition index (n) was computed directly from the V-I characteristics of the wire in the electric field range of about 1-10 $\mu\text{V}/\text{m}$ as the wire enters the resistive transition. The index is defined empirically by the relationship $V \propto I^n$.

Table 1. Design details of the composites studied

Composite designation	Manufacturer	Nb-Ti rod condition in extrusion billet	Design filament dia. at 0.0318" wire diameter	Received composite diameter	Nb barrier cross section ratio
1836-1	OST	Annealed	6 μm	1.04(in)	1%
1837-2	OST	Cold Worked	9 μm	1.04	1
2096-1	Supercon	Cold Worked	9 μm	0.86	2
2096-2	Supercon	Cold Worked	6 μm	0.86	2
5263-2*	IGC	Cold Worked	20 μm	1.03	2
5263-3	IGC	Cold Worked	20 μm	1.03	2

* designates the ternary Nb-41.5Ti-15Ta Fermi Quadrupole conductor.

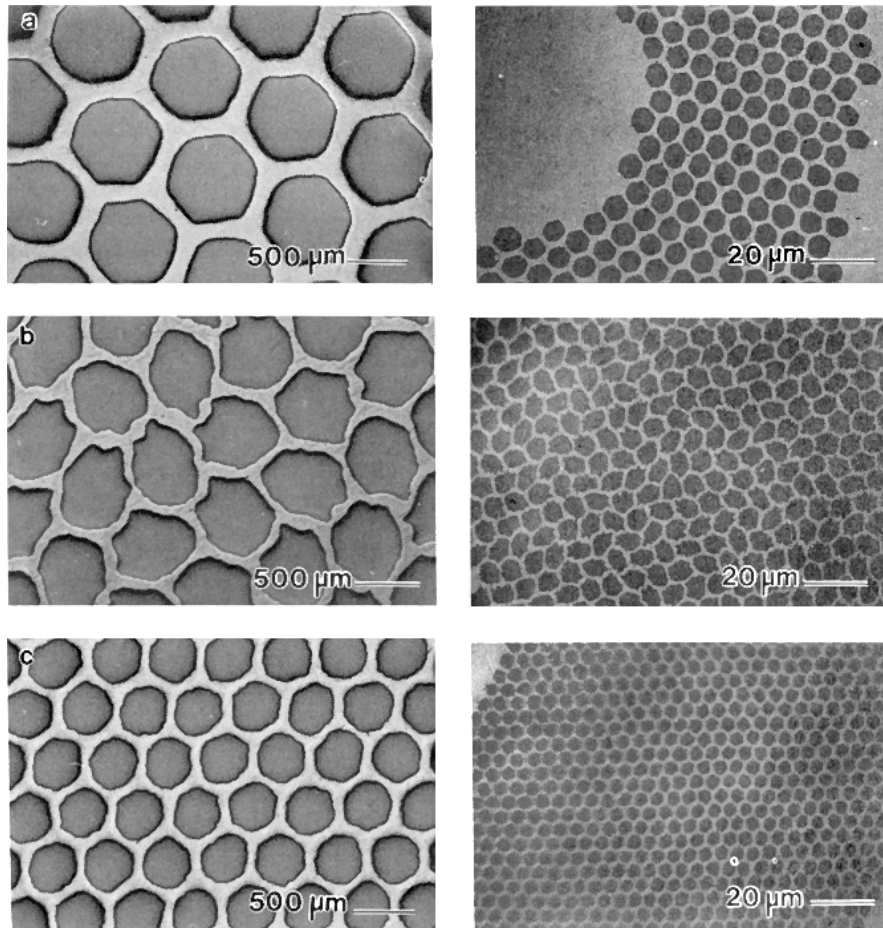


Fig. 1. Transverse cross sections of composites at 0.6" and 0.0318" wire diameters a.) 5263.3.C (20 μm filaments) b.) 2096.1.C (9 μm filaments) c.) 1836.1.C (6 μm filaments).

RESULTS

Examples of typical cross sections are shown in fig. 1. There is a general deterioration in filament shape and variation as the filament size diminishes, irrespective of manufacturer. Thus the 20 μm filament conductor (all filament sizes are expressed at a wire diameter of 0.0318" unless otherwise noted.) has excellent quality, whether examined at 0.6" or 0.0318" (Fig. 1a). The 2096 series conductors show irregular-shaped filaments at both sizes. The 6 μm filament shape was quite regular but was markedly more variable in cross-section than the larger filament conductors and shows the greatest deterioration with decreasing size.

These points are expressed more quantitatively in figures 2 and 3. Fig. 2 compares the effect of heat treatment on one of the 9 μm composites (2096.1). σ_{n-1}/\bar{A} is clearly much larger for the "real" optimization heat treatments B and C, as compared to the "gentle" anneal of heat treatment A. σ_{n-1}/\bar{A} was 3.5-4% after the second heat treatment rising to about 5 % for heat treatment A and about 7.5% for heat treatment B and C. It is particularly evident that the principal filament damage occurs during the final drawing strain. A more global view for all composites is shown in Fig. 3a. (B heat treatment) and 3b. (C heat treatment). For the B heat treatment the final size σ_{n-1}/\bar{A} varied from 5 to 9 %, the dispersion being least for the 20 μm and greatest for the 6 μm conductors. Exactly the same was true for the C heat treatment, except that the dispersion was significantly larger, being 6-7 % for the 20 μm filament conductors and 10-13% for the 6 μm filament conductors. Thus there is a clear general tendency for the more aggressive heat treatment to produce the greater damage. However, this is much more marked for the 6 μm than for the 9 or 20 μm composites.

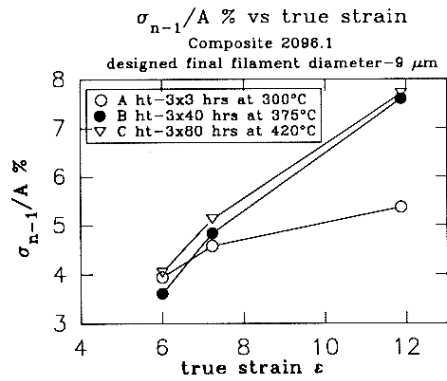


Fig. 2 σ_{n-1}/\bar{A} versus fabrication strain for 2096.1 9 μm filament conductor for 3 different heat treatment schedules.

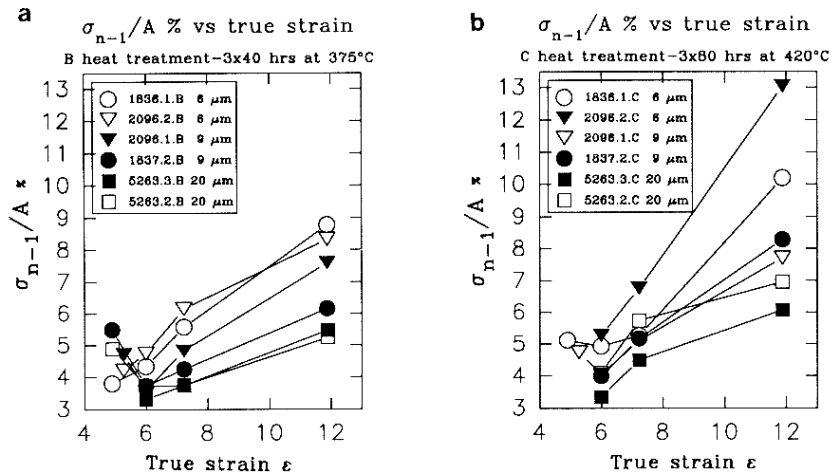


Fig. 3 σ_{n-1}/\bar{A} versus fabrication strain for all composites for a.) the B heat treatment b.) the C heat treatment

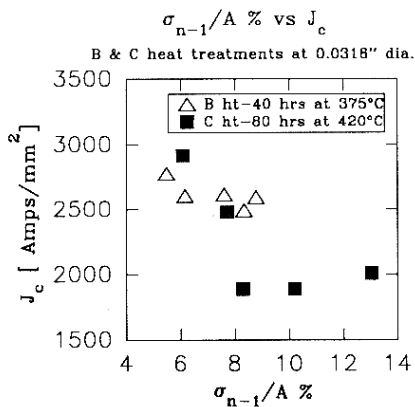


Fig.4 σ_{n-1}/\bar{A} versus J_c for the B and C heat treatments at 0.0318" diameter.

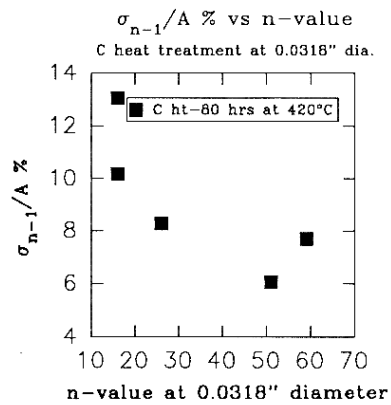


Fig.5 σ_{n-1}/\bar{A} versus n-value for the B and C heat treatments at 0.0318" diameter.

The effect of this filament non-uniformity on the superconducting properties is shown in Figs. 4 and 5. Figure 4 plots J_c (5T, $10^{-14}\Omega\cdot m$) at 0.0318" dia. vs. σ_{n-1}/\bar{A} . J_c falls rapidly as σ_{n-1}/\bar{A} increases. The effect is much more marked for the aggressive C heat treatment which initially had the highest J_c . Recalling that the effective SSC specification is $2750 A/mm^2$ underlines the importance of raising the intrinsic J_c as high as possible and then ensuring that the transport critical current density, J_{ct} , is not degraded by filament sausaging. Thus only 2 out of the 10 wires in Fig. 4 meet the specification. Figure 5 plots the n -value against σ_{n-1}/\bar{A} . Given that individual n values have an uncertainty on the order of $\pm 20\%$, a scatter band is more appropriate than a single line fit. There is a clear correlation with an n value of 20 at 5 Tesla corresponding to σ_{n-1}/\bar{A} of 12 % while n of 50-60 corresponds to 6-8% dispersion. Over the range considered, the two variables appear to be inversely proportional.

A final connection can be made to the filament surface quality. SEM micrographs of the exposed filaments show that there is an increase in the frequency of intermetallic nodules present as the measured σ_{n-1}/\bar{A} increases. Figure 6a shows the exposed filaments from composite 2096.2.C at the 6 μm filament size. Many nodules are visible, as is the total sausaging associated with them (σ_{n-1}/\bar{A} of 13%). Figure 6b. shows that composite 2096.1.C with a 9 μm filament size and a measured σ_{n-1}/\bar{A} of 8 % has very few nodules. It is interesting that the nodule in the central filament appears to "erupt" from under the barrier. Indeed there is a somewhat swollen band associated with the nodule, which extends along the filament. This is consistent with the conclusion of Faase et al.¹³ that the principal reacted layer occurs under the barrier. Finally, fig. 6c. shows the exposed filaments for the 5263.3.C composite with 20 μm filaments. These filaments are very clean and their measured σ_{n-1}/\bar{A} is 6%.

DISCUSSION

Higher and longer heat treatment temperatures and times produce filament non-uniformity as a result of intermetallic formation at the filament-Cu interface. The measured σ_{n-1}/\bar{A} values coupled with the SEM analysis of the exposed filaments show clearly that more intermetallic is directly associated with higher σ_{n-1}/\bar{A} values. The factors most directly controlling the intermetallic formation are the time and temperature of final size heat treatment and the thickness of the barrier at that size, as discussed by Faase et al.¹³ This is particularly evident for the filaments subjected to the more rigorous C heat treatment. The gentle A heat treatment (Fig.2), however, shows the best results by having a very low σ_{n-1}/\bar{A} of 3.5 % at 0.6" dia., this only increasing to 5.5% at 0.0318" dia. By contrast the same 9 μm filament composite had a filament

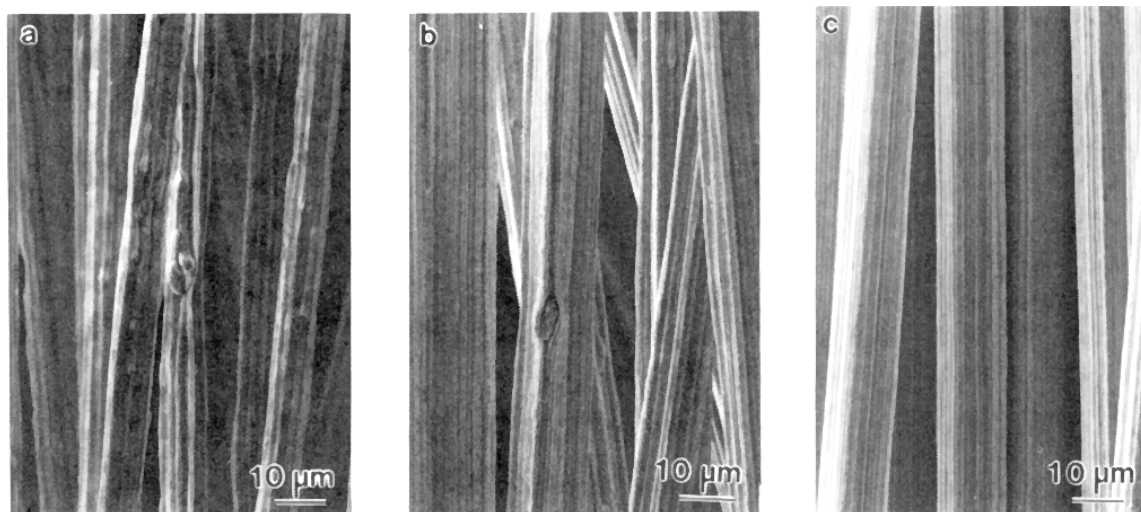


Fig 6. SEM micrographs showing exposed filaments of a.) 6 μm dia.(1836.1.C) b.) 9 μm dia.(2096.1.C) c.) 20 μm dia.(5263.3.C) taken at final composite diameter of 0.0318".

non-uniformity of almost 8% for the "real" heat treatments A and B. For the thick barrier 20 μm filament conductor, filament uniformity was somewhat better, 5-6% for heat treatments B and C. This is the same as seen for the gentle heat treatment B on the 9 μm filament conductor. Thus a non-uniformity of 5-6% may be typical of the particular local area ratios now being chosen for SSC composites. The differences in σ_{n-1}/\bar{A} became dramatic for the 6 μm filament conductors: for the B heat treatment they reached 8-9 %, while attaining 10 and 13 % for the C heat treatment. It is also interesting that the most non-uniform barrier was not one with a 1% barrier, but the irregularly shaped 2096.2.C composite. Nb barriers do not deform uniformly and it appears that the irregular filament shape is particularly detrimental to barrier quality. Thus maintaining filament quality requires thick enough barriers to inhibit diffusion and the formation of intermetallic nodules that impede the uniform deformation of the filaments. 2% barriers are not good enough to protect 6 μm filaments for all heat treatments.

Comparison of the J_{ct} measurements with σ_{n-1}/\bar{A} shows the changeover from intrinsic to extrinsic control of the J_c which occurs as the filaments sausage. The more aggressive heat treatment C initially shows a higher J_{ct} than the B heat treatment, but this rapidly disappears as the filament quality degrades.

CONCLUSIONS

1. Quantitative image analysis shows that the filament non-uniformity, expressed as σ_{n-1}/\bar{A} increases slowly with increasing strain, until such point that the Nb barrier on the filaments is compromised. After this point degradation is rapid.
2. Filament irregularity increases with longer and higher heat treatment times and temperatures. The higher heat treatment temperatures and durations permit more intermetallics to grow and these control the sausageing.
3. Transport critical current density declines strongly as the measured σ_{n-1}/\bar{A} increases.

ACKNOWLEDGEMENTS

We are grateful to William Starch, Kenny Faase, Alex Squitieri and Rick Noll for experimental assistance. Supply of composite material by R.M. Scanlan (LBL), D. Capone (SSC) and A.D. McInturff (FNAL) is greatly acknowledged. This work was supported by the SSC laboratory and the DOE-Office of High Energy Physics, Grant #DE-AC02-82ER-4007.

REFERENCES

- 1 H. C. Kanithi, C. G. King, B. A. Zeitlin and R. M. Scanlan, IEEE Trans. Mag. 25:1922-1925 (1989).
- 2 E. Gregory, T. S. Kreilick, J. Wong, E. W. Collings, K. R. Marken Jr., R. M. Scanlan and C. E. Taylor, IEEE Trans. Mag. 25:1926-1929 (1989).
- 3 S. Hong, D. Geschwindner, A. Manatone, W. Marancick, S. Zalek, and R. Zhou, IEEE Trans. Mag. 25:1934-1936 (1989).
- 4 D. C. Larbalestier, Li Chengren, W. Starch and P. J. Lee, IEEE Trans. NS. (1985).
- 5 H. Hillman, Superconductor Materials Science, p.275, Ed. 1.
- 6 M. Garber, M. Suenaga, W. B. Sampson, R. L. Sabatini, IEEE Trans.NS. (1985).
- 7 D. C. Larbalestier, P. J. Lee, R.W. Samuel, Adv. Crvo. Eng. 32:715 (1986).
- 8 R. M. Scanlan, J. Royet, and R. Hannaford, IEEE Trans.Mag. 23:1719 (1987).
- 9 D. C. Larbalestier, IEEE Trans.Mag. 21:257 (1985).
- 10 W. H. Warnes and D. C. Larbalestier, Cryogenics 26:643 (1986).
- 11 W. H. Warnes, J. Appl. Phys. 63(5): 1651 (1988).
- 12 J. Ekin, Cryogenics, 27:603-607 (1987).
- 13 K. J. Faase, P. J. Lee, J. C. McKinnell, and D. C. Larbalestier, Adv. in Cryo. Eng. 38: 723-730 (1992).
- 14 P. J. Lee, J.C. McKinnell, and D.C. Larbalestier, Adv. Cryo. Eng., 36:287-296 (1990).
- 15 Li Chengren and D.C. Larbalestier, Cryogenics 27:171 (1987).